Available online at www.sciencedirect.com
ScienceDirect
Journal of Colloid and Interface Science 320 (2008) 501–507
JOURNAL OF Colloid and Interface Science
www.elsevier.com/locate/jcis

Preparation and characterization of hydrophobic TiO_2 pillared clay: The effect of acid hydrolysis catalyst and doped Pt amount on photocatalytic activity

Xuejun Ding [a,d], Taicheng An [a,*], Guiying Li [a], Shanqing Zhang [b], Jiaxin Chen [a,d], Jianmei Yuan [c], Huijun Zhao [b], Hui Chen [c], Guoying Sheng [a], Jiamo Fu [a]

[a] *State Key Laboratory of Organic Geochemistry, Guangdong Key Laboratory of Environmental Resources Utilization and Protection, Guangzhou Institute of Geochemistry, Chinese Academy of Sciences, Guangzhou 510640, China*
[b] *Australian Rivers Institute and Griffith School of Environment, Gold Coast Campus, Griffith University, QLD 4222, Australia*
[c] *School of Chemistry and Chemical Engineering, Northwest Normal University, Lanzhou 730070, China*
[d] *Graduate School of Chinese Academy of Sciences, Beijing 100049, China*

Received 30 August 2007; accepted 29 December 2007

Available online 14 February 2008

Abstract

Titanium hydrate sols were prepared using different acid hydrolysis catalysts, i.e., acetic acid and hydrochloric acid. The platinum-doped TiO_2 sol–gels were also synthesized by adding K_2PtCl_6 into the titanium hydrate sols. The hydrophobic montmorillonite clay, treated with organic cationic surfactant, i.e., hexadecyltrimethylammonium bromide, was used as a template to prepare TiO_2 pillared photocatalyst with the above sols. Scanning electron microscopy (SEM), X-ray diffraction (XRD) and energy dispersive X-ray analysis (EDX) were employed to characterize the resulting photocatalysts. The adsorption performance and photoactivity of prepared pillared clays were studied by using methyl orange as a model organic pollutant. The preliminary results indicated that the hydrophobic TiO_2 pillared clay prepared with acetic acid as the acid hydrolysis catalysts possessed higher photocatalytic activity than that with hydrochloric acid. Due to the excellent sedimentation property of the clay, the resulting pillared photocatalyst is easily recovered and reused in the postrun treatment. Also the doping of platinum into the hydrophobic photocatalyst can increase the photocatalytic activity significantly.

Keywords: Pillared clay; Photocatalyst; Platinum; Preparation; Characterization

1. Introduction

In the past few years, the introduction of organic or inorganic cations into layered materials, such as montmorillonite, has been developed to prepare various porous pillared materials. Numerous articles have been reported to use semiconductor pillars to prepare new combined functional clays. The photocatalytic activities of the synthetic clay with semiconductor pillars, such as supported TiO_2 and Fe_2O_3, were much higher than those of unsupported catalysts [1–3]. But these pillared catalysts have low adsorption capability when it is applied to the treatment of trace organic pollutants in water. An effective solution is to enhance the hydrophobicity of the photocatalyst. This can be realized by improving the hydrophobicity of the clay layer exchanged with cationic organic surfactant, which can improve the adsorption capacity of organic pollutants markedly.

The intercalation of TiO_2 into the interlayer of clays is one of the most promising methods for synthesizing TiO_2 pillared clays and for improving the photocatalytic activity for the degradation of organic pollutants in water. The TiO_2 pillared clays can be synthesized from hydrochloric acid containing TiO_2 sol [4], $TiCl_4$–ethanol solution [5] and TiO_2 sol with organic acid such as acetic acid [6] and oxalic acid [7]. During the hydrolysis reaction, the pH value will change radically when HCl is added as a hydrolysis catalyst, which may result in the

* Corresponding author. Fax: +86 20 85290706.
E-mail address: antc99@gig.ac.cn (T. An).

0021-9797/$ – see front matter
doi:10.1016/j.jcis.2007.12.042

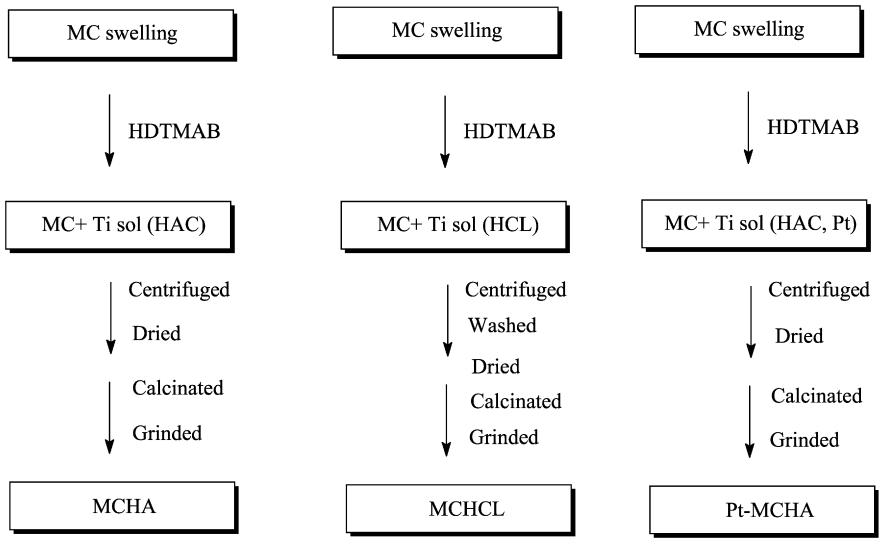

Chart 1. Synthesis process of pillared clay materials.

formation of large particle sizes of the TiO_2 catalyst and subsequently affects the pillaring reaction and morphology of the pillared structure. The hydrolysis reaction can be better controlled when acetic acid is used to replace HCl, leading to small TiO_2 particle sizes [7].

In order to increase the adsorption capacity and photocatalytic activity, the hydrophobic TiO_2 pillared clays were synthesized in this work. The organic surfactant hexadecyltrimethylammonium bromide (HDTMAB) was added into the hydrolysis reaction medium at the initial preparation step to increase the hydrophobicity of the target materials. Acetic acid and hydrochloric acid were used as two different acid media to prepare titania sol gels that were subsequently used to compare the photocatalytic activity of titanium dioxide pillars. The adsorption capacity and photocatalytic activity of the two prepared hydrophobic TiO_2 pillared clays with different acid hydrolytic catalysts for the degradation of methyl orange (MO) were investigated, respectively. It is well established that the doping of some precious metals, such as platinum (Pt), can significantly increase the photocatalytic activity of titanium dioxide [8,9]. To our knowledge, no work has been done to investigate the effect of precious metals on the photocatalytic activity of TiO_2 pillared clay. For the first time, we tried to improve the photocatalytic activity by applying the precious metal to pillared clay photocatalyst.

2. Experimental

2.1. Materials and apparatus

The raw montmorillonite clay (MC) was collected in Lin'an, Zhejiang, China. The weight chemical composition was measured as (SiO_2) 57.13%, (Al_2O_3) 17.31%, (MgO) 3.11%, (CaO) 1.78%, (Fe_2O_3) 1.65%, (Na_2O) 2.32%, (K_2O) 0.38%, (MnO) 0.03%, (H_2O) 6.95%, and other ingredients 9.16%. The MC powder has a specific surface area of 18.03 $m^2\,g^{-1}$, which was tested by a nitrogen adsorption and desorption method. Its cation-exchange capacity (CEC) is 54.47 mmol/100 g. Titanium tetraisopropoxide was purchased from Ghangzhou Chemical Reagents Factory, China, and used without further purification to prepare titanium hydrate sol. Other chemical reagents, including hexadecyltrimethylammonium bromide, acetic acid, hydrochloric acid, potassium hexachloroplatinate (K_2PtCl_6), and organic dye MO, were of analytical grade.

XRD patterns were measured using a Rigaku D/Max 2200 VPC powder diffractometer with Cu$K\alpha$ radiation ($\lambda = 0.15418$ nm), accelerating voltage of 40 kV, emission current of 30 mA, and scanning speed of 10° min^{-1} was used to determine the crystal phase composition of the prepared materials at room temperature. Scanning electron microscope (SEM, LEO 1530 VP) was used to observe the crystal microstructure and size of the prepared pillared clays. The composition of the pillared clays was characterized by energy-dispersive X-ray analysis (EDX, GENESIS-2000). The specific area of raw clay powder was measured by a NOVA-1000 single sample surface area and pore size analyzer. The concentration of MO reaction solution was examined by a UV–vis spectrophotometer (Thermo Spectronic, Heλios-α).

2.2. Synthesis of pillared clays

The synthesis routes of three types of pillared clays are presented in Chart 1. Accordingly, three types of titanium hydrate sols were first prepared. Route 1: The first titanium hydrate sol (Ti Sol HAc) was prepared by the addition of titanium tetraisopropoxide into CH_3COOH aqueous solution. The molar ratio of $Ti(OC_3H_7)_4$:CH_3COOH:H_2O was 1:10:40. Route 2: The second titanium hydrate sol (Ti Sol HCl) was prepared in HCl solution with a molar ratio of $Ti(OC_4H_9)_4$:HCl:H_2O 1:10:40. Route 3: The third sol (Ti Sol HAc-Pt), i.e., hydrophobic Pt-doped TiO_2 pillared catalysts, were synthesized by adding various amount of K_2PtCl_6 solid powder into the Ti sol originating from acetic acid (i.e., Ti sol HAc) with Pt concentrations of 0.1, 0.2, and 1.0% (w/w).

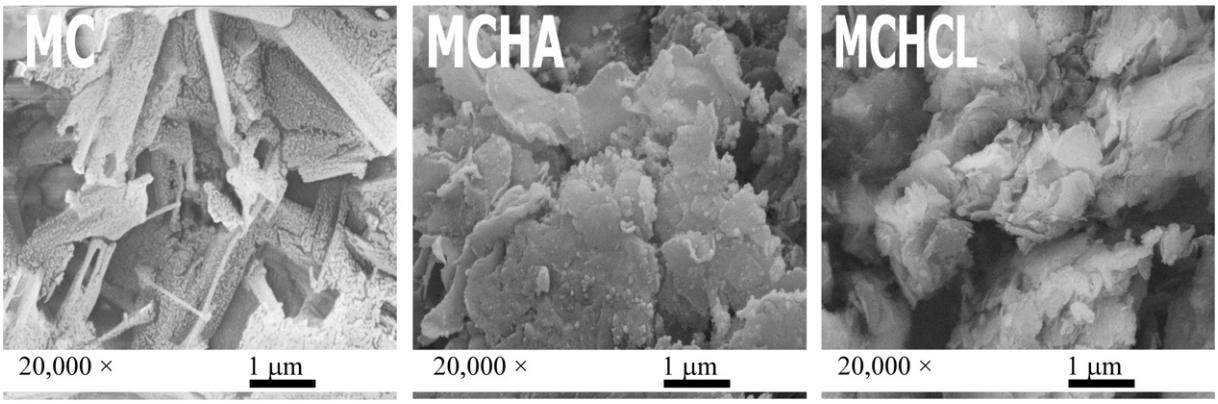

Fig. 1. SEM micrographs of raw MC, MCHA, and MCHCL clays.

The raw MC was ground into powder and sieved through a 200-mesh screen. The sieved powder was added into water to form a 1% (w/w) aqueous suspension. This aqueous suspension was kept at room temperature for 24 h to swell the clay. The swelled clay was pretreated with HDTMAB by a cation-exchange process with a HDTMAB to a CEC molar ratio of 2:1. After 4 h of aging of the above sols, the Ti sols were dropped slowly into the swelled clay mixture with molar ratio of Ti:CEC 40:1 following different routes as shown in Chart 1.

These mixtures resulting from the three routes were stirred for another 48 h to obtain three solid suspensions. Individually, the solid suspensions were centrifuged, washed with deionized water to remove excessive acetic acid or HCl, dried thoroughly at a temperature of 333 K in an oven, calcinated at 723 K for 4 h, and then ground into powder. Subsequently, three types of surfactant-pretreated TiO_2 pillared MC catalysts were obtained. The TiO_2 pillared MC sample using acetic acid as hydrolysis media (Route 1) was labeled as MCHA, while sample prepared in HCl solution (Route 2) as MCHCL. The hydrophobic Pt-doped TiO_2 pillared clay sample (Route 3) was named as Pt-MCHA (see Chart 1).

2.3. Adsorption and photodegradation of MO

The adsorption and photocatalytic degradation experiments of an organic dye MO were carried out in a double-wall cylindrical quartz reactor (150 ml). The double wall was used as a thermostat jacket to keep the temperature of solutions constant throughout all experiments. A 125 W high-pressure mercury lamp (GGZ300, Shanghai Yaming Lighting Co., Ltd., $E_{max} = 365$ nm) was installed at a side wall of the photoreactor to provide irradiation. Prior to photodegradation, the suspension of 150 ml MO (20 mg dm^{-3}) containing 0.3 g pillared clay catalyst was stirred in the dark for 30 min to establish an adsorption/desorption equilibrium between dye and catalyst. At a given time interval, 5 ml MO reaction solution was sampled and filtered with a membrane (pore size 0.22 μm). The filtrates were analyzed using a UV–vis spectrophotometer at a wavelength of 464 nm, the maximum adsorption wavelength for MO.

3. Results and discussion

3.1. The characterization of the photocatalysts

3.1.1. SEM images

Fig. 1 shows representative SEM photographs of the MC, MCHA, and MCHCL samples. The MC has a structure of abundant layers and nanopores. This microstructure of the clay was retained in the MCHA after calcinations at high temperatures. In contrast, no micropores and interlayer structure can be found in the MCHCL sample, which maybe due to the strong acidity of HCl. This result suggests that titanium sol originating from acetic acid can keep the pristine microstructure much better than that from hydrochloric acid. Compared with HCl, the hydrolysis reaction of $Ti(OC_4H_9)_4$ could be slowed down due to the use of the weak acetic acid [10], which will result in the formation of smaller, uniform titanium hydrate and fine TiO_2 particles during this hydrolysis period after exchange reaction with ions in the interlayer of raw clay. In the case of the HCl media, its much stronger acidity leads to the rapid hydrolysis reaction of $Ti(OC_4H_9)_4$, which resulted in a large particle size. Furthermore, a poisonous effect can be expected due to the adsorption of chloride ions on the TiO_2 surface [11].

SEM images of Pt-MCHA with different Pt doping amount are shown in Fig. 2. The original layered and microporous structure of MC was retained better in Pt-MCHA pillared clays than in MCHA (see Fig. 1). The organic surfactant HDTMAB can act as a dispersing medium to maintain the layered structure during the reactions and the subsequent high temperature calcination. It can also be observed that the layered structure of Pt-MCHA (1.0% Pt) is much better retained than the other two Pt-MCHA samples (i.e., 0.1% Pt, 0.2% Pt). This phenomenon may be due to the increment of ionic strength resulting from the addition of K_2PtCl_6, which is beneficial to the ion-exchange reaction between the organic surfactant cations in the interlayer of the MC. Consequently, the pillared structure was well maintained, and a greater adsorption capacity can be expected for the synthesized hydrophobic clays.

3.1.2. Specific surface area (BET)

The specific surface area of these samples was measured in this study. The specific areas of MCHA and MCHCL were 94.2

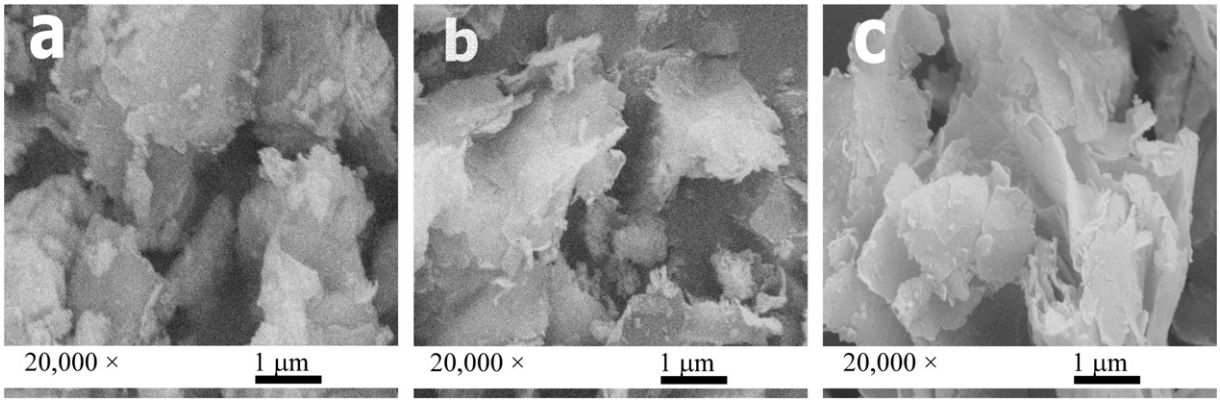

Fig. 2. SEM micrographs of Pt-MCHA pillared clays (a: 0.1%; b: 0.2%; c: 1.0% Pt).

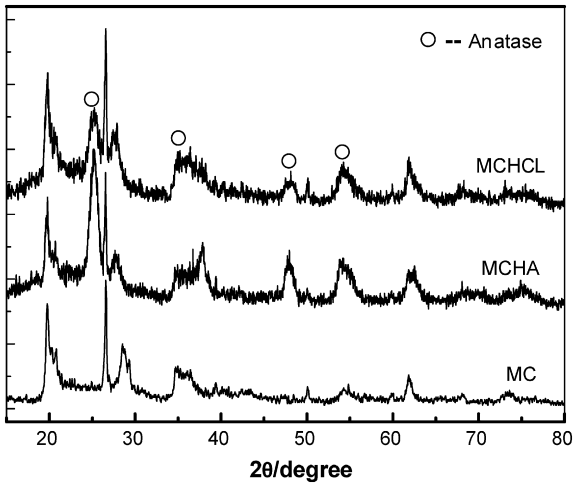

Fig. 3. XRD patterns of raw MC, MCHA, and MCHCL clays.

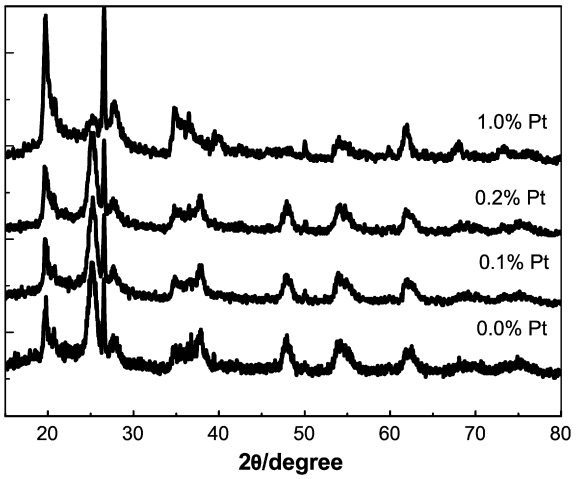

Fig. 4. XRD patterns of different Pt-MCHA clays.

and 96.5 $m^2\,g^{-1}$, respectively. This is in strong contrast with the raw MC, which has a relatively small specific surface area of 18.0 $m^2\,g^{-1}$. This suggested that organic surfactant pretreatment and titanium dioxide pillars affect the microstructure and the surface area of the MC dramatically. This can be a significant indication that the modified clays will possess enhanced adsorption capacity for wastewater treatment.

The specific surface areas of Pt-MCHA samples (0.1, 0.2, 1.0% Pt) are 79.4, 80.2, and 59.3 $m^2\,g^{-1}$, respectively. It indicates that the specific surface areas of all Pt-modified MCHAs are smaller than those of MCHA (94.2 $m^2\,g^{-1}$). These suggest that the Pt modification decreases the specific surface area significantly, and that the adsorption capability of Pt-MCHA will be lower than that of MCHA.

3.1.3. XRD results

Fig. 3 shows powder X-ray diffraction patterns of the MC, MCHA, and MCHCL samples. Generally, the anatase phase TiO_2 can be determined from the characteristic adsorption peaks at a 2θ of 25.3, 37.9, 47.6, and 54.8° [12]. No typical adsorption peaks of the anatase phase TiO_2 were observed in the raw MC. In contrast, all four characteristic anatase peaks appeared in the XRD patterns of MCHA and MCHCL clay, which indicates that the anatase phase TiO_2 has been successfully intercalated into the clays. The average sizes of the anatase TiO_2 particles in two pillared clay samples were calculated by the broadening of the most intensive X-ray diffraction peak at $2\theta = 25.3°$ (101) using the Debe–Scherrer equation [13]. The average sizes of the anatase crystals of MCHA and MCHCL pillared clay are 11.7 and 12.7 nm, respectively.

The XRD patterns of the four Pt-MCHA pillared clays are shown in Fig. 4. The four characteristic anatase peaks can be observed for these samples. The average sizes of TiO_2 calculated using the Debe–Scherrer equation are 11.7, 12.3, 12.5, and 12.7 nm for 0, 0.1, 0.2, and 1.0% Pt in the pillared clay samples. This suggests that the average size of TiO_2 is not affected significantly by the content of Pt.

3.1.4. EDX analysis

In our previous work [14], the Pt element could not be observed in the X-ray photoelectron spectra (XPS) pattern of Pt-doped titanium dioxide nanoparticle (1.0% Pt) samples except the elements carbon, oxygen, and titanium. It could be due to a few reasons: (a) the low concentration of Pt ions [15]; (b) XPS used for the measurement is not sensitive enough; (c) the penetration of Pt element into the skeleton of TiO_2. To verify the actual existence of Pt, the energy dispersive X-ray spectrometer experiment was carried out and the result is seen in

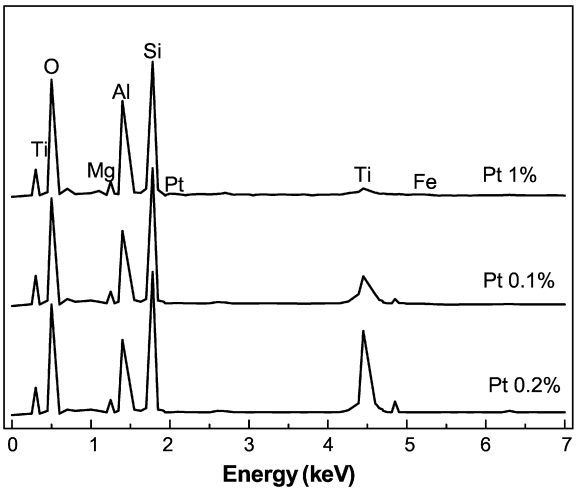

Fig. 5. EDX spectra of different pillared clays.

Fig. 5. A weak peak due to Pt element was observed only in the 1.0% Pt-doped MCHA sample, and no corresponding peak in the other two Pt-MCHA pillared clay samples (0.1 and 0.2% Pt). As suggested above, the EDX result confirmed the existence of Pt in prepared pillared clays and this precious metal is difficult to detect at low contents when compared to other elements.

3.2. Adsorption and photocatalytic degradation of MO

The adsorption and photocatalytic degradation kinetics of MO using MCHA and MCHCL as photocatalyst (2 g dm^{-3}) are given in Figs. 6 and 7, respectively. It can be seen that the pillared catalysts pretreated with organic surfactant have better adsorption capability to MO as shown in Fig. 6. The adsorption equilibrium was achieved within 20 min in room temperature. The amount of MO adsorbed on different samples can be figured out clearly. Just about 10.0% of starting concentration of MO was adsorbed by the MC sample, while 26.4 and 25.2% of MO were adsorbed on MCHA and MCHCL, respectively. These results also confirm the results of BET and SEM. It is well known that the adsorption of organics from water on adsorbents is not only influenced by the specific surface area but also affected by the hydrophobicity or the polarity of adsorbents. Since water is preferentially adsorbed on hydrophilic clay matrix, its surface should be hydrophilic. When the clay was modified with organic surfactants, its surface will become more hydrophobic and possess larger adsorption capacity to organic pollutants.

The comparison of photoactivity between MCHA and MCHCL is seen in Fig. 7. All photochemical experiments were conducted under the same conditions after the adsorption equilibrium was achieved. As shown in Fig. 7, we can see that the photolysis efficiency of MO is slow and only 29.6% was degraded within 1 h in distilled water. The photocatalytic activity of two prepared pillared clays, MCHA and MCHCL, is much higher than photolysis of MO. Within identical reaction duration, 82.7 and 79.1% of MO were photocatalytically degraded by MCHA and MCHCL, respectively. It can be concluded that

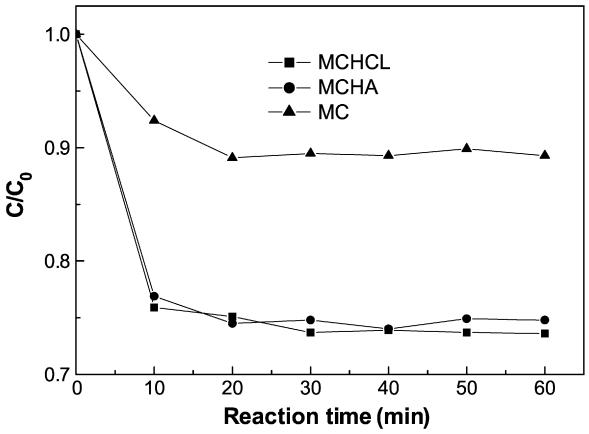

Fig. 6. Adsorption kinetics of MO on MC, MCHA, and MCHCL pillared clays.

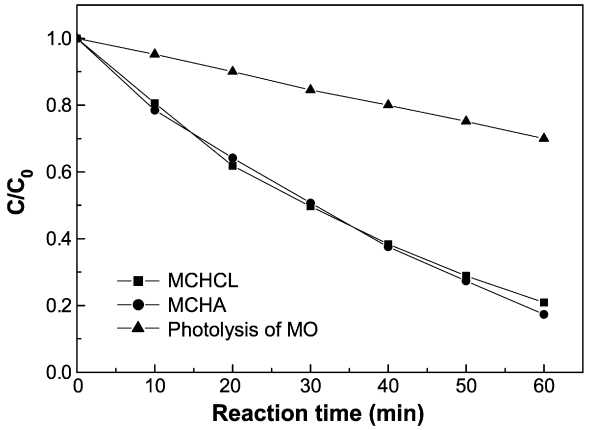

Fig. 7. Photolysis of MO and photocatalytic degradation of MO on MCHA and MCHCL pillared clays.

the prepared hydrophobic TiO_2 pillared clays have good photoactivity, which has also been suggested by anatase TiO_2 peaks in XRD graphs. This confirmed that Ti sol originating from acetic acid can lead to better crystallized anatase titanium dioxide as noted above.

3.3. Recovery of photocatalyst

Because, the photocatalytic degradation reaction takes place on the surface of titanium dioxide particles, the fine catalyst powders with large surface-to-volume ratios normally possess a satisfactory efficiency in aqueous solution during the enhanced mass transport. However, the recovery of the photocatalyst from the aqueous solution after treatment has always been a critical problem [16]. This is mainly due to the high cost of separating the titanium catalyst particles from the aqueous system. Furthermore, the separation process would make the treatment very complicated [16]. This hindered the large-scale industrial application of TiO_2-based technology. It is well known that clay has much better sedimentation properties than P25, a commonly available commercial TiO_2 [3]. This implies that the clay-based photocatalyst recycling can be potentially achieved by simple precipitation. This is an important and useful property of the clay, especially in a scale-up system. The hydrophobic TiO_2 pil-

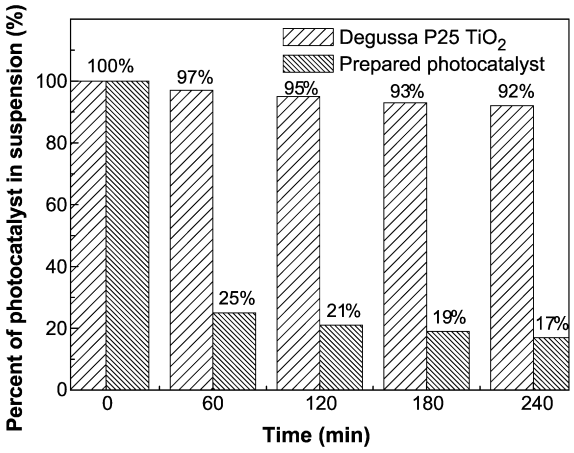

Fig. 8. The comparison of the precipitation percentage between Degussa P25 TiO_2 and prepared photocatalyst.

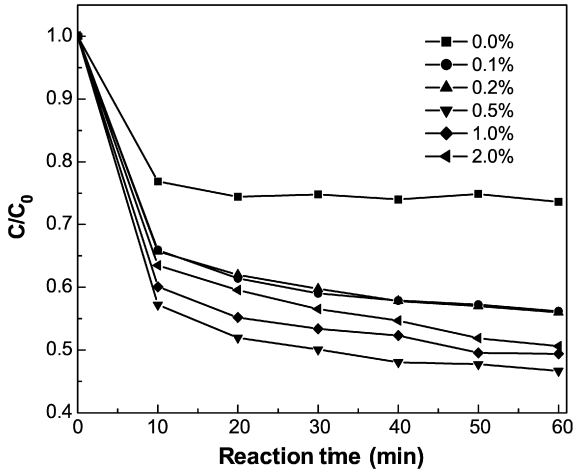

Fig. 9. Adsorption kinetics of MO using different Pt-MCHA pillared clays as adsorbents (the Pt concentration is indicated in the figure).

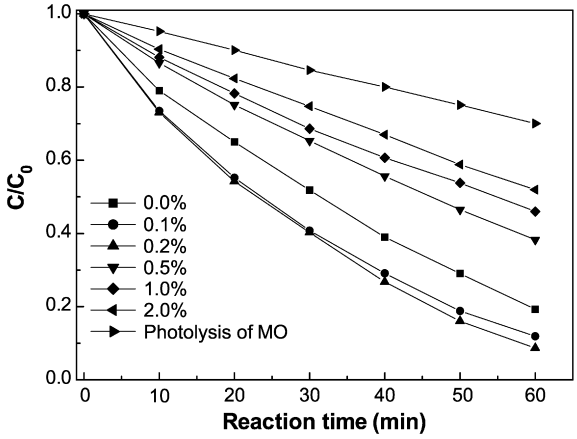

Fig. 10. Degradation kinetics of MO using different Pt-MCHA pillared clays as catalysts (the Pt concentration is indicated in the figure).

lared MC was prepared by introducing the titanium ions into the clay layer. Thus, these MC photocatalysts would possess good sedimentation properties from the water. In order to investigate the sedimentation character and the feasibility of photocatalyst recovery using this sedimentation property, we have also studied the recovery of a suspended MCHA photocatalyst from solution. The photocatalyst with a concentration of 2 $g\,L^{-1}$ in slurry system was contained in a measuring cylinder for the photocatalyst recovery experiment. The weight and recovery efficiency of the photocatalyst in supernatant can be calculated by microfiltration and thorough drying of the solid phase. At fixed intervals, the precipitate is removed from suspended solution and the supernatant was assessed by the standard suspended solid measurement method [17] and the experimental results represented as the sedimentation percentage of used photocatalyst are shown in Fig. 8. It can be seen that the hydrophobic TiO_2 pillared montmorillonite photocatalyst (MCHA) has better precipitation performance than Degussa P25 TiO_2. Within the tested 240-min period, Degussa P25 TiO_2 photocatalysts have no apparent sedimentation. Only 3 and 8% Degussa P25 TiO_2 were deposited from the suspended solution at intervals of 60 and 240 min, while 75 and 83% of the MCHA were settled from the suspension within the identical intervals. Especially in the first 60-min interval, the prepared photocatalyst settles dramatically, and then gradually changes. Thus, the hydrophobic TiO_2 pillared montmorillonite photocatalyst has much higher recovery efficiency than a traditional photocatalyst, i.e., Degussa P25 TiO_2, which suggests that the former can be more suitable in wastewater treatment.

3.4. The effect of Pt-doped amount on the adsorption and photocatalytic activity

Low photocatalytic efficiency due to the fast recombination of photogenerated electron and hole has been a major concern in the application of TiO_2 photocatalytic process. Contact of precious metal with the semiconductor can indirectly influence the energetics and interfacial charge transfer process in a favorable way [18]. Semiconductor–metal composite nanoparticles facilitate charge (electron) stabilization and improve the photoefficiency in the system. The noble metal deposition is improved to be an effective approach to increase the activity of prepared photocatalysts. The experiments of adsorption and photocatalytic degradation of MO were carried out with different contents of Pt-doped MCHA under the same conditions as noted above. The result shown in Fig. 9 indicated that the different additions of Pt can also influence the adsorption capability of synthesized clays. All adsorption equilibria were achieved in starting 20 min. The adsorption capacity increased for doped clay from 0 to 0.5% Pt and decreased gradually with further addition of Pt. It can be found that the doping of precious metal Pt can enhance the electrostatic interaction with the electron-rich centers of the dye due to the positive charge on these metal ions [19]. On the other hand, the hybrid structure of Pt may have strong oxidation potential and results in the partial oxidation of MO under dark conditions already. More effort should be dedicated to further investigation.

The effect of different concentrations of Pt on the photocatalytic activity of Pt-MCHA clays is seen in Fig. 10. The degradation rate of MO increased with the increment of Pt concentration from 0 to 0.2% and then decreased slightly later. About 91.3% of MO has been photocatalytically degraded by

Pt-MCHA (0.2% Pt) and only 48.1% MO was degraded by Pt-MCHAc (2% Pt). This can be interpreted that when the doping percentage of Pt is moderate, the dopant Pt can act as electron trapping sites to prolong the lifetime of the electrons and holes and subsequently reduce the recombination of the electrons and holes generated in a semiconductor when illuminated by UV light. However, too many trapping sites on the surface of the photocatalyst will lead to a shorter distance among the trapping sites, which may become the recombination center conversely and accelerate the recombination of electrons and holes [20]. Also the excessive doping amount of Pt can decrease the effective mass transport between the TiO_2 and the degradation substrate (e.g., MO) or block some effective UV illumination on the TiO_2 surface. These may all contribute to the decrease of photocatalytic activity for the excessive Pt-doping catalyst.

4. Conclusions

Novel hydrophobic TiO_2 pillared clays were prepared in different pathways, including $Ti(OC_4H_9)_4$ hydrolysis in different acid media and doping of TiO_2 with different Pt concentrations. The treatment of surfactant HDTMAB in the synthesis process can increase the hydrophobicity of the pillared clays and the adsorption capability to organic dye MO significantly. The hydrophobic TiO_2 pillared clays produced from the Ti sol prepared in acetic acid (i.e., MCHA) possess higher photocatalytic activity than that in hydrochloric acid (i.e., MCHCL). The hydrophobic TiO_2 pillared montmorillonite photocatalyst can be recovered easily at the postrun treatment and reused in the consecutive treatment due to its excellent sedimentation performance. The doping of precious metal Pt enhances the photoactivity of the hydrophobic TiO_2 pillared clays further. According to the experiments results, 0.2% (w/w) of Pt is an optimal Pt concentration for the hydrophobic TiO_2 pillared clays. The resulting catalyst was able to degrade 91.3% of MO within 60 min.

Acknowledgments

The authors appreciate the financial support from the National Nature Science Foundation of China (Nos. 40302013 and 40572173), and the Nature Science Foundation of Guangdong Province, China (No. 030466) and the Science and Technology Project of Guangdong Province, China (Nos. 2006A36701002 and 2005A30401001), are also gratefully acknowledged.

References

[1] Y. Fujishiro, S. Uchida, T. Sato, Int. J. Inorg. Mater. 1 (1999) 67.
[2] Y. Kitayama, T. Kodama, M. Abe, H. Shimotsuma, Y. Matsuda, J. Porous Mater. 5 (1998) 121.
[3] P.R. Mishra, P.K. Shukla, A.K. Singh, O.N. Srivastava, Int. J. Hydrogen Energy 28 (2003) 1089.
[4] Z. Ding, H.Y. Zhu, G.Q. Lu, P.F. Greenfield, J. Colloid Interface Sci. 209 (1999) 193.
[5] G.R.R.A. Kumara, K. Tennakone, V.P.S. Perera, A. Konno, S. Kaneko, M. Okuya, J. Phys. D Appl. Phys. 34 (2001) 868.
[6] C. Guillard, D. Debayle, A. Gagnaire, H. Jaffrezic, J.M. Herrmann, Mater. Res. Bull. 39 (2004) 1445.
[7] G.X. Tang, R.J. Zhang, Y.N. Yan, Z.X. Zhu, Mater. Lett. 58 (2004) 1857.
[8] A.L. Linsebigler, G.Q. Lu, J.T. Yates, Chem. Rev. 95 (1995) 735.
[9] A.V. Vorontsov, E.N. Savinov, Z.S. Jin, J. Photochem. Photobiol. A 125 (1999) 113.
[10] J.M. Yuan, T.C. An, H. Chen, J. Chen, X.J. Ding, G.Y. Sheng, J.M. Fu, J. Funct. Mater. 36 (2005) 477, in Chinese.
[11] M. Abdullah, G.K.C. Low, R.W. Matthews, J. Phys. Chem. 94 (1990) 6820.
[12] S. Yamanaka, T. Nishihara, M. Hattori, Y. Suzuki, Mater. Chem. Phys. 17 (1987) 87.
[13] H.P. Klug, L.E. Alexander, X-Ray Diffraction Procedures for Polycrystalline and Amorphous Materials, Wiley, New York, 1974, p. 618.
[14] H. Chen, J.M. Yuan, M.L. Zhang, J.X. Chen, T.C. An, G.Y. Sheng, J.M. Fu, J. Saf. Environ. 5 (2005) 1.
[15] G. Facchin, G. Carturan, R. Campostrini, S. Gialanella, L. Lutterotti, L. Armelao, G. Marci, L. Palmisano, A. Sclafani, J. Sol–Gel Sci. Technol. 18 (2000) 29.
[16] H.Y. Zhu, Y. Lan, X.P. Gao, S.P. Ringer, Z.F. Zheng, D.Y. Song, J.C. Zhao, J. Am. Chem. Soc. 127 (2005) 6730.
[17] EPA of China, The Methods for Water and Wastewater Monitoring and Analysis, third ed., Environmental Technology and Science Press of China, Peking, 1989, p. 108.
[18] P.V. Kamat, J. Phys. Chem. B 106 (2002) 7729.
[19] K. Wilke, H.D. Breuer, J. Photochem. Photobiol. A 121 (1999) 49.
[20] O. Carp, C.L. Huismanb, A. Rellerb. Prog. Solid State Chem. 32 (1–2) (2004) 33.